



The light triggered dissolution of gold wires using potassium ferrocyanide solutions enables cumulative illumination sensing

Weida D. Chen^a, Seung-Kyun Kang^b, Wendelin J. Stark^a, John A. Rogers^{c,d,e}, Robert N. Grass^{a,*}

^a Department of Chemistry and Applied Biosciences, ETH Zurich, Vladimir-Prelog-Weg 1, 8093 Zurich, Switzerland

^b Department of Bio and Brain Engineering, KAIST, 291 Daehak-ro, Yuseong-gu, Daejeon 334141, Republic of Korea

^c Departments of Materials Science and Engineering, Biomedical Engineering, Neurological Surgery, Chemistry, Mechanical Engineering, Electrical Engineering and Computer Science, Northwestern University, Evanston, IL 60208, USA

^d Center for Bio-Integrated Electronics, Northwestern University, Evanston, IL 60208, USA

^e Simpson Querrey Institute for Nano/Biotechnology, Northwestern University, Evanston, IL 60208, USA

ARTICLE INFO

Keywords:

Photochemistry
Cyanide
Sensor
Conductors
Diffusion limitation
Devices

ABSTRACT

Electronic systems with on-demand dissolution or destruction capabilities offer unusual opportunities in hardware-oriented security devices, advanced military spying and controlled biological treatment. Here, the dissolution chemistry of gold, generally known as inert metal, in potassium ferricyanide and potassium ferrocyanide solutions has been investigated upon light exposure. While a pure aqueous solution of potassium ferricyanide–K₃[Fe(CN)₆] does not dissolve gold, an aqueous solution of potassium ferrocyanide–K₄[Fe(CN)₆] irradiated with ambient light is able to completely dissolve a gold electrode within several minutes. Photo activation and dissolution kinetics were assessed at different initial pH values, light irradiation intensities and ferrocyanide concentrations. Addition of small amounts of the heavy metal thallium (260 ppb) also provides tunability of the dissolution kinetics. An investigation of the involved chemical and physical processes of photochemistry, cyanide diffusion and surface reaction results in an understanding of the rate limiting steps and yields an overall transformation of irradiated light energy to dissolved gold of 2.6%. A potential application of this novel gold dissolution method as a cumulative light sensor is demonstrated and discussed.

1. Introduction

To achieve a maximal reliability and stability, most electronic devices depend on inert metals such as gold, silver and platinum for conductors as they offer optimal chemical stabilities in combination with excellent electronic conductivities. In contrast thereto, transient electronics give devices new functions by dissolving or destroying the device within a programmed timeframe or on-demand control via chemical interaction [1–9]. This type of electronics can provide bioresorbable medical devices without the need of extraction surgery, environmental friendly green-devices without electrical waste, and hardware based security and military electronic systems without exposing important information to unknown targets. Transient electronics use certain metals (magnesium (Mg), zinc (Zn), iron (Fe), tungsten (W) and molybdenum (Mo)), as they degrade/dissolve in deionized water and physiological solutions [10–12].

Specifically, gold is known as a material for electrical conduction (electronics industry demand of 6% of the global gold production; first

quarter 2017) [13] due to its unique physical attributes (high stability/conductance, low elasticity modulus and low yield point) and its ability to maintain a good connectivity whilst being exposed to hostile environments for an extended period of time [14]. As a result, gold is widely used as a connecting element in personal computers and other electronic devices. As gold is seen as one of the most noble and most chemically resilient metals, gold circuitry is usually not considered when seeking electronic devices that intrinsically interact with their chemical environment, or have any other transient functionality.

However, some known chemical reactions provide a chance to dissolve gold under given conditions, which may be applied to transient electronics: The MacArthur-Forrest process, which is commonly referred to as gold cyanidation and patented in 1887, was first commercially applied in the Crown Mine in New Zealand and is still used in the gold mining industry today. This method takes advantage of the strong binding of the cyanide ion CN⁻ to gold in aqueous solution [15]. The dissolution reaction of gold in cyanide solution, also known as Elsner equation, is a redox reaction involving oxygen and water:

* Corresponding author.

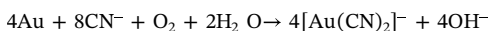
E-mail address: robert.grass@chem.ethz.ch (R.N. Grass).

<https://doi.org/10.1016/j.snb.2018.10.094>

Received 25 May 2018; Received in revised form 17 October 2018; Accepted 20 October 2018

Available online 02 November 2018

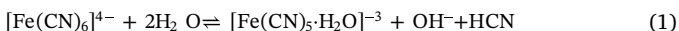
0925-4005/ © 2018 Elsevier B.V. All rights reserved.



In addition to gold, other metals such as copper (Cu), iron (Fe), nickel (Ni), silver (Ag) and zinc (Zn), all of them currently used in electronic devices, are dissolvable in cyanide solution. The downside of this extraction technique is its acute toxicity, not only to humans but also to wildlife [16–18]. The fabrication of interactive electronic devices essentially containing gold wiring would thus require a source of free cyanide ions, which until now pose a high risk to the environment due to the readily available state of the cyanide ion. With this restriction in mind we proceeded to look for non-toxic cyanide containing precursors, which exhibit cyanide release upon external triggering or any physical change in the environment.

Potassium ferricyanide $\text{K}_3[\text{Fe}(\text{CN})_6]$ and potassium ferrocyanide $\text{K}_4[\text{Fe}(\text{CN})_6]$ are considered strong metal-cyanide complexes with an oral LD_{50} value for rats of 1600–3200 mg/kg, which is in a similar range to sodium chloride [19]. The stable nature of these cyanide containing iron complexes is well studied. Depending on the pH, Meeussen et al. projected half-lives ranging from 1 year (reducing conditions) to 1000 years (oxidizing conditions) at pH 4, demonstrating that strong acidic conditions are required to dissociate these complexes, releasing the cyanide [20].

Already in 1905 Fritz Haber published a study on the stability of potassium ferrocyanide and reported that light exposure can result in free cyanide [21]. The dissolution reaction of potassium ferrocyanide has since then been investigated more intensely, and one of the proposed reactions is formulated in Eq. (1) [22].

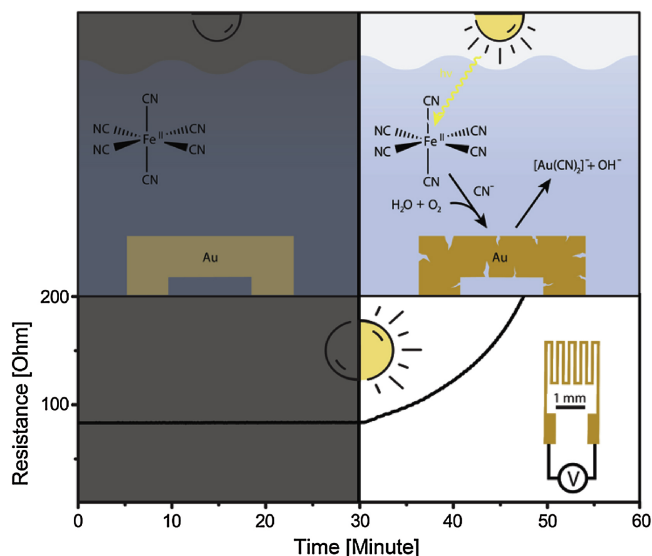


Similarly, potassium ferricyanide has been shown to release cyanide upon illumination, with reports of even higher cyanide generation release rates [23]. This literature inspired us to investigate the light induced dissociation of cyanide from those precursors and combining this photochemistry with the dissolution of a gold electrode shown in Scheme 1.

2. Materials and methods

2.1. Gold electrode fabrication

Cr/Au (2 nm/80 nm) deposited by electron beam-evaporation (Cr: 0.1 nm s^{-1} , Au: 1 nm s^{-1} , Plassys II) were patterned by photolithography (AZ1518 photoresist, 4000 rpm, 45 s, Karl Süss MA6) onto



Scheme 1. Photo-initiated cyanide release followed by gold cyanidation. Resistance monitored over 60 min.

a glass substrate previously cleaned using Piranha acid (24 h). After developing (AZ726), excessive Cr/Au etched and photoresist washed off using acetone, then rinsed with deionized water and dried with N_2 . Photoresist residues cleaned in O_2 plasma (5 min, 150 W).

2.2. Fabrication of full device

PDMS ratio 1:10 (30 g total, Sylgard 184, Dow Corning) was mixed (1 min, 3500 rpm, DAC 150 FVZ, Speed Mixer) with black silicon colorant (0.1 g, PMS black, Smooth-On). After degassing in high vacuum, silicon was poured into mold fabricated from Teflon enclosed in aluminum frame and cured with polycarbonate lid at 80°C for 4 h. Final dimensions of the whole device were $11 \times 6 \times 10 \text{ cm}$ (length \times width \times height) each device containing 12 gold serpentes. The gold electrode device and PDMS sample holder were exposed to oxygen plasma (60 s, 50% Power, Diner Electronics), both aligned and pressed tightly together for 10 s, baking at 80°C for 4 h. A picture of the device is included in supplementary information in Fig. A1.

2.3. Solution preparation

Resistance measurements were carried out in $\text{K}_4[\text{Fe}(\text{CN})_6]$ solution ($\text{K}_4[\text{Fe}(\text{CN})_6] \cdot 3\text{H}_2\text{O}$, $\geq 98.5\%$, Sigma-Aldrich) and KCN solution ($\geq 98\%$, Fisher). Buffers with pH 3, 4 and 5 contained acetic acid ($> 99.8\%$, Sigma-Aldrich) and sodium acetate ($> 99\%$, Acros Organics), pH 6–10 buffers were made with tris(hydroxymethyl)aminomethane ($\geq 99.8\%$, Biosolve) and hydrochloric acid (37.2%, Merck), pH 11 buffer was made with $\text{NaH}_2\text{PO}_4 \cdot 4\text{H}_2\text{O}$ (Merck) and NaOH ($\geq 97.0\%$, Fisher Chemical), pH 12 and 13 buffers were made with KCl ($\geq 99.5\%$, Sigma-Aldrich) and NaOH ($\geq 97.0\%$, Fisher Chemical).

2.4. Light exposure

For achieving a controlled light environment, an Oriel Class A Solar Simulator (91195A, Newport) was operated at 450 W, light intensities were adjusted using fine metal meshes, measurements of light intensities were performed with an Oriel PV Reference Cell System (Model 91150 V, Oriel Instruments), and samples were placed in the middle of the lens 14 cm away from the source. The spectrum is included in the supplementary information in Fig. A2. Measurements were always performed with a 2 mm thick Quartz glass (Suprasil 1/D, Wisag) on top of the reaction chambers to prevent evaporation and ensure maximum transparency for wavelengths down to UV range (long pass cut at 170 nm).

2.5. Characterization

Resistance data were retrieved using a Multifunction I/O device (USB-6001, National Instruments) operated over LabVIEW, voltage change across a known resistance (10 kOhm) and the sample resistance in series were recorded and the resistance calculated as shown in Figs. A3 and A4.

Free cyanide concentration was measured using a standardized gas test (Hydrocyanic Acid 0.5/a, Draeger). A sample volume of 1 mL was pipetted in a glass vial, after adding $10 \mu\text{L}$ of a 0.1 M HCl solution, the gas phase was pumped through the tube and a color change could be observed if hydrogen cyanide was present (Fig. A5).

Scanning electron microscope (Nova Nano SEM 450, FEI) pictures were taken after sputtering (25 s at 60 mA, EM SCD 005, Leica) a 5 nm layer of Pt. Optical microscope pictures were taken on an optical microscope (Axio Imager.M2m, Zeiss).

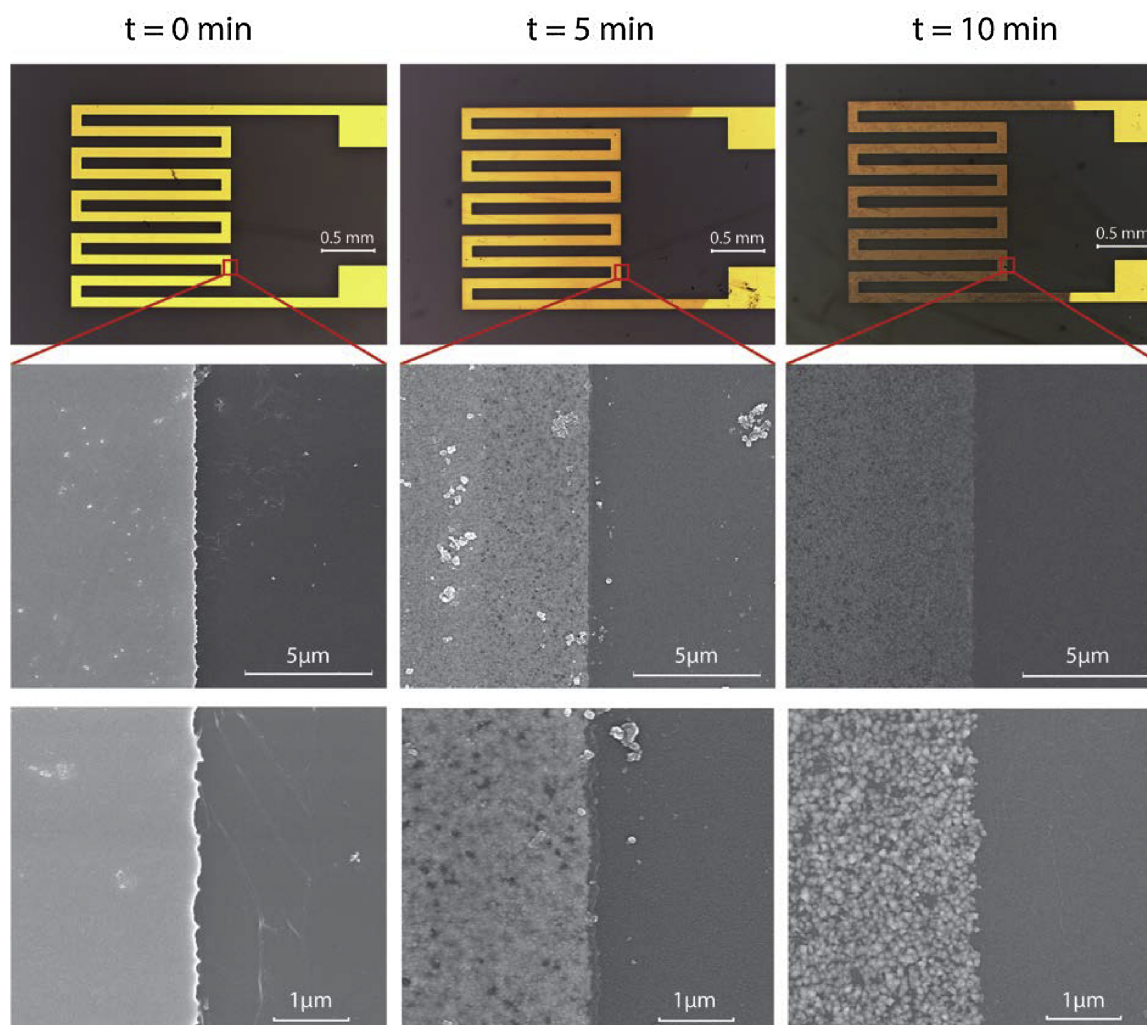


Fig. 1. Light microscope and SEM pictures of the gold surface before, after 5 and 10 min of illumination. Dissolution is progressing with increasing illumination time.

3. Results and discussion

3.1. Proof of concept

In first experiments gold serpentine structures were immersed in saturated potassium ferrocyanide solutions ($c_{\text{sat}} = 0.93 \text{ mol L}^{-1}$ at RT) in the dark, without any observable effects, even after long immersion times. However, when the immersed samples were irradiated with ambient light for various durations dissolution of the gold structures could be observed via optical and electron microscopy. The concentration was chosen to maximize photon-complex interaction. The immersed gold structures shown in Fig. 1 exhibit an increasing degree of gold dissolution with increased immersion time, visible at the edges of the borders where after 10 min of immersion the bottom structure of the glass slide was becoming visible.

With the visual confirmation of gold being dissolved, and in order to get a more quantitative reading, the serpentine was connected to an I/O multimeter aiming to monitor dissolution kinetics through the change in resistance of the dissolving gold wire (Scheme 1). The initial resistance measured for the samples was $80 \pm 2 \text{ Ohm}$, using Pouillet's law shown in Eq. (2) the resistivity of the deposited gold material was obtained at 35.8 nOhm m .

$$\rho = \frac{RA}{l} \quad (2)$$

With this data and assuming homogeneous gold deposition from

electron-beam (E-beam) evaporation, a correlation between layer thickness and resistance could be plotted, which assisted in the subsequent comparison and calculation of gold dissolution rates in various chemical environments (Fig. A6).

The following experiment aimed to assess whether both potassium ferrocyanide (Fe^{2+}) and potassium ferricyanide (Fe^{3+}) are capable of dissolving gold, since both complexes have been described in literature as able to dissociate free cyanide ions upon illumination [23]. However, when the gold resistor was immersed in each solution, both at a concentration of 0.5 mol L^{-1} and exposed to an irradiance of 350 W m^{-2} , the resistance only increased in the case of potassium ferrocyanide, shown in Scheme 1 and Fig. A7. As a result, ferricyanide was seen as non-photoreactive with gold (in the scope of interest), and all following experiments were conducted with potassium ferrocyanide.

From our current understanding and by comparing potassium ferrocyanide and potassium ferricyanide, it is not sufficient for a cyanide containing compound to dissociate upon irradiation. Under our experimental conditions, the critical step of gold dissolution was only possible with potassium ferrocyanide. Currently potassium ferrocyanide seems to be the only compound to satisfy both criteria of photoactivity and gold dissolvability. Nevertheless, other hexacyano compounds such as potassium hexacyanochromate (III) or tetracyano compounds such as potassium tetracyanonickelate (II) might be of interest, but were not tested due to the potential toxicity of the heavy metals [24,25].

In order to test if the photodegradation of ferrocyanide to yield free

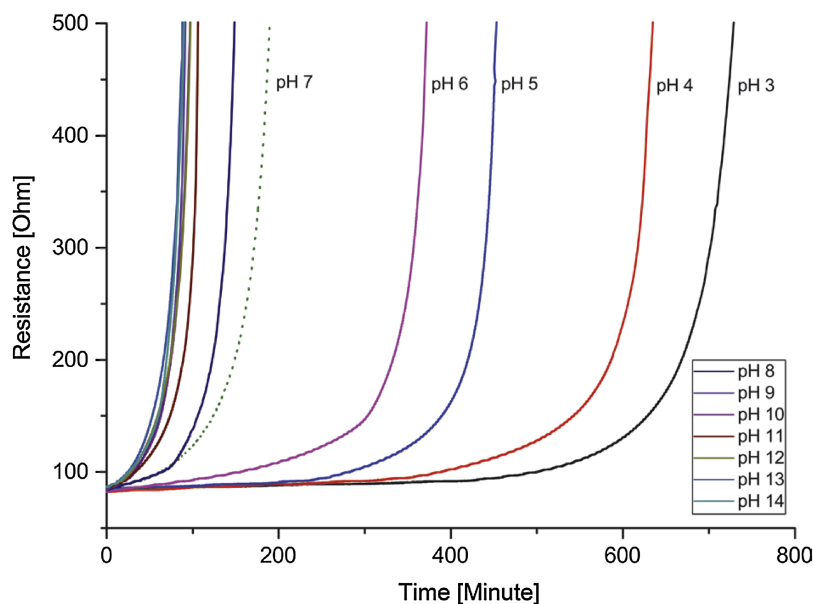


Fig. 2. Different initial pH values do not interfere with the photo-initiated release of cyanide. pH values higher than 7 are known to be favorable for cyanidation reactions and can be observed here as well.

cyanide ions would be a feasible explanation of the observed gold dissolution, cyanide generation was independently measured from irradiated and non-irradiated ferrocyanide solutions. For this gas phase method was utilized instead of standard UV/VIS assays as the light source would interfere with the control experiment requiring absolute darkness. Indeed, in the absence of light, no detectable cyanide was formed, independent of pH, temperature and heavy metal addition, and optical irradiation could be identified as the sole experimental parameter required to generate free cyanide ions from ferrocyanide (see Figs. S5 and S7).

3.2. Effect of pH on cyanide release

In order to investigate the effect of pH on the photoreaction, gold dissolution experiments in ferrocyanide solutions were carried out at constant optical irradiance and different initial pH values ranging from pH 3 to 14 (Fig. 2). In the acidic range a strong increase of the reaction rate with increasing initial pH could be observed. This increase saturated at ca. pH 9, at which further increasing the basicity did not result in an acceleration of the reaction. This observation is in accordance with literature and can be explained by the high pK_a value of hydrogen cyanide at 9.21, resulting in less free cyanide ions in acidic pH solutions to react with gold on the surface. Therefore, the presence of ferrocyanide does not have any influence on the pH dependency of the gold cyanidation reaction.

Furthermore, standard gold leaching industry utilizes calcium oxide (CaO) to maintain a stable alkaline pH at 9–10 aiming to achieve maximum gold leaching rates [26,27]. Looking more carefully at the data at lower initial pH, it can be seen that at, e.g. pH 3 the reaction starts very slowly (or even has a lag-time compared to the other data), but in the end reacts just as fast as experiments conducted at high initial pH. The reason for this can be found in Eq. (1), which not only describes the light induced formation of cyanide, but also describes the formation of hydroxide ion (OH^-) by photodissociation of ferrocyanide. As a consequence, it can be concluded that at low initial pH the photochemical reaction (1) is active, but has to first generate sufficient OH^- before the gold cyanidation reaction picks up and starts to dissolve the gold.

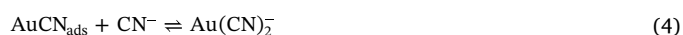
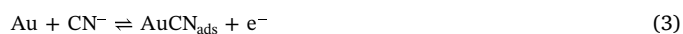
This is further confirmed by measuring the pH values after the reaction, which all ranged from 9–11, regardless of initial pH. In order to not be susceptible to this pH dependent effect, all following

experiments were conducted under constant pH, just above the literature value, at pH 12. After testing several buffer systems, this was best achieved using the buffer (NaOH/KCl), which managed to keep the pH constant throughout the reaction. In order to show that the utilized buffer and chlorine source [28] cannot induce cyanide formation or gold dissolution in comparable timeframes, corresponding control experiments were performed (Figs. S5 and S7).

3.3. Concentration dependence of gold dissolution

Different concentrations of free cyanide (CN^-) from a KCN solution and cyanide bound to the complex $[\text{Fe-CN}]$ from our ferrocyanide solution were compared at the same molarities ranging from 2.5 to 125 mmol L^{-1} . This range was chosen based on literature values, which suggest an optimum gold conversion at a free cyanide concentration between 1.1 and 6.0 mmol L^{-1} [27]. Potassium cyanide (KCN) was also taken into the study to establish a reference point in order to approximate the quantity of free cyanide in solution set free via photoactivation of ferrocyanide. In addition to varying concentrations, different irradiation intensities were investigated and both dependencies are shown in Fig. 3.

For better comparison between the KCN reference and potassium ferrocyanide, first analysis utilized the slope of the resistance change at minute 10 to estimate the overall reaction rate. For the reference material KCN the cyanidation rate increased with increasing KCN concentrations up to 25 mmol L^{-1} , and then declined at even higher initial cyanide concentrations. This is in agreement with current mechanistic theories of surface reactions where either adsorption, reaction or desorption are rate limiting. Gold cyanidation is an electrochemical process, which involves an oxidative surface reaction described by Equation 3 and Equation 4 [29].



Another reaction on the gold surface has also been proposed, as given in Eq. (5).



Generally, the theory has been accepted that a solid polymeric layer of AuCN_{ads} or an adsorbed layer of AuOH_{ads} forms on the gold surface,

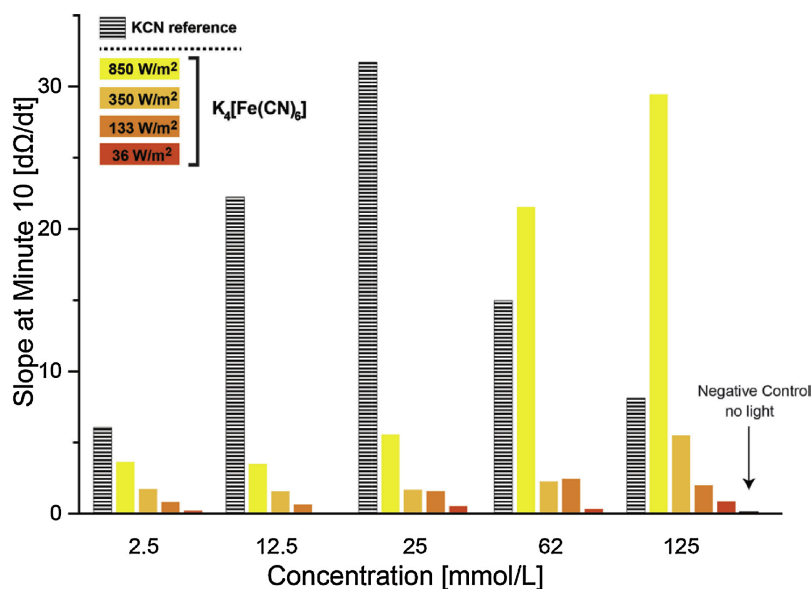


Fig. 3. Rate of resistance increase of a gold wire comparing potassium cyanide and light induced ferrocyanide gold leaching at various initial concentrations of cyanide generating species and light intensities (buffered at pH 12). The rate of the nonlinear signal change was quantified after 10 min of reaction to be able to compare the various conditions. Measurements were conducted once for each condition and concentration. Error bars were omitted; errors for the measurements are within 2%.

slowing down the reaction [30–32]. A high initial cyanide concentration results in more extensive coverage of the passivation compounds, thus resulting in a decrease of the reaction rate.

For the case of potassium ferrocyanide, the rate of resistance increase (gold dissolution) increased with both irradiation intensity and initial potassium ferrocyanide concentration, in accordance with general photochemistry theory. As the gold dissolution rates of 125 and 62 mmol L⁻¹ ferrocyanide at 850 W m⁻² are comparable to the potassium cyanide data at 25 and 12 mmol L⁻¹, respectively, it can be extrapolated that under these conditions ca. 1/5 of the original ferrocyanide has decomposed to form free cyanide according to equation (1). The fact that ferrocyanide can outperform potassium cyanide at 125 mmol L⁻¹ initial concentrations can be attributed to the surface saturation argument given above.

For a better understanding and interpretation of the irradiation intensity, data at initial ferrocyanide concentrations of 25 mmol L⁻¹ were plotted for different illumination intensities ranging from 850 to 36 W m⁻² in Fig. 4a. This time the resistance data was converted to a calculated gold layer thickness using Pouillet's law shown in Eq. (2).

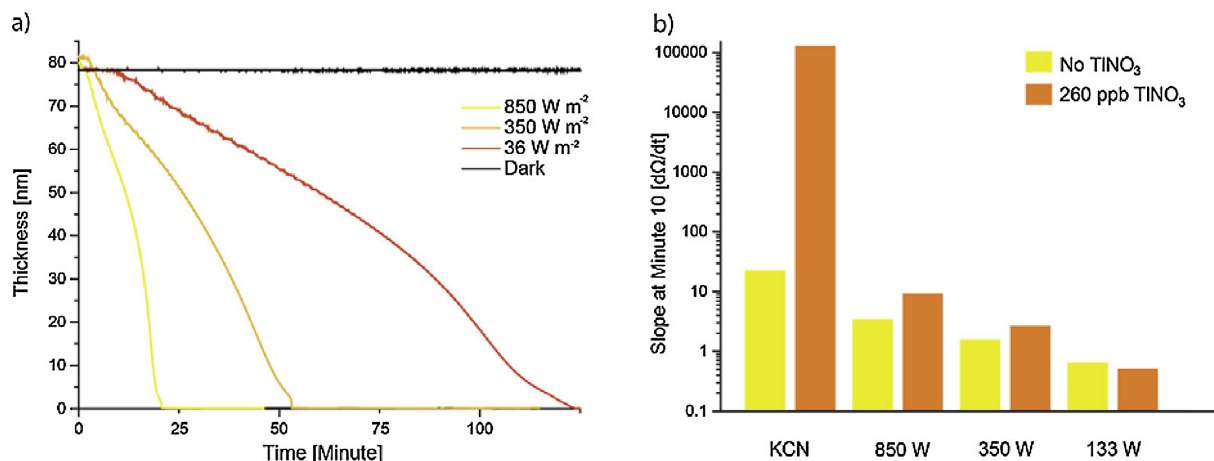


Fig. 4. (a) Four different irradiation intensities which were assessed, all with the same ferrocyanide concentration of 25 mmol L⁻¹ and buffered at pH 12. This plot demonstrates the illumination intensity dependence of the light triggered dissolution process. One reference sample, same conditions but kept in complete darkness, did not show any measurable change in thickness. (b) Effect of thallium on the cyanidation rate. The initial concentration of potassium cyanide and ferrocyanide were both 12.5 mmol L⁻¹. While the addition of thallium increased the cyanidation in KCN at a rate 5000×, the increase was not as significant for potassium ferrocyanide, indicating that in this case the rate determining step is not the gold dissolution as such, but rather the cyanide generation reaction (especially at lower light intensities). Error bars were omitted; errors for the measurements are within 2%.

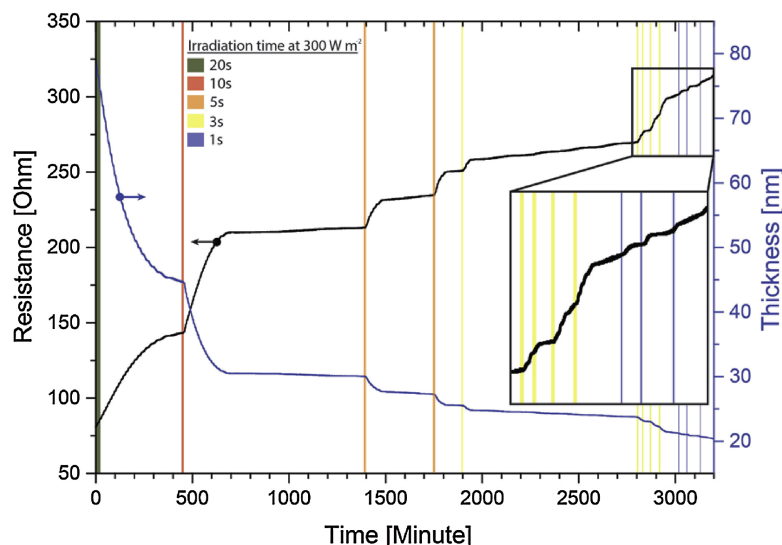


Fig. 5. Demonstration of application of a gold layer immersed in an aqueous solution of ferrocyanide as a simple cumulative light sensor. Illumination duration was changed from 20 to 1 s to test the range, response time and sensitivity of the sensor.

If thallium was added to the photoreaction, the effect of the heavy metals was also observable, however not to quite the same extent. This data verified that the ferrocyanide dissolution system was not as susceptible to the AuCN_{ads} passivation layer, suggesting that a gradual in situ generation of free cyanide was more favorable for the cyanidation reaction.

Finally, the system was assessed under periodic light exposures with a constant illumination intensity of 300 W m^{-2} (Fig. 5). Illumination times were chosen accordingly to test the full-range sensitivity of the system; by having longer exposure times in the beginning, more gold was degraded leading to an increased sensitivity. The demonstration device showed that gold dissolution correlates with the illumination time. Upon stoichiometric comparison, an illumination duration of 20 s degrades approximately 35 nm of gold, whereas an illumination of 10 s leads to a thickness reduction of 15 nm. From the generated data the sensitivity of the system can be extrapolated to being able to measure a 1 s irradiation with 300 W m^{-2} (equivalent of exposure of the sensor to full sunlight for one second at noon in January in Switzerland) [34].

In Table 1 a summary of other light quantification methods, which work either in a cumulative manner or are based on photoconductive principles is presented. Photochromic molecules, reversible or irreversible, can be used to quantitatively measure light exposure. The downside of this technique is the analysis via UV/VIS measurement in order to be quantitative. However, the visual assessment can sometimes be enough to determine whether light exposure took place. On the other hand, photoconductive elements such as light dependent resistors (LDR), photodiodes, phototransistors and photovoltaic cells exhibit

excellent and robust light measurement properties with instant signal readout. However, in order to be cumulative the measurement needs to be logged by an external device. Fig. A8 shows a schematic of a direct comparison between a light dependent resistor and the light triggered gold cyanidation sensor. The photo activated cyanidation system can detect small energies in a cumulative manner, the overall response rate however, is relatively slow (time of light pulse until new steady state was reached, ca 5 h, see Fig. 5). This slow reaction rate can be attributed to the diffusion limitations of cyanide in the reaction volume (Fig. 6): Free cyanide formed during the photochemical degradation of ferrocyanide would have to diffuse through the whole reaction chamber, which had a filling height of 5.5 mm. Assuming a CN^- diffusion coefficient of $1.6 \times 10^{-3} \text{ mm}^2 \text{ s}^{-1}$, this characteristic diffusion time from top to bottom would be 315 min, which well describes the systems response time and indicates that an optimization of the reaction chamber to allow for thinner ferrocyanide films would result in a more rapid response. Taking this diffusion time into consideration, the light triggered gold degradation system has been divided into three determining steps (Fig. 6): First, the generation of cyanide is a prerequisite for the reaction to take place, this process is strongly dependent on the illumination intensity and duration (irradiation energy) as well as the concentration of the ferrocyanide in the solution. Second is the diffusion of the generated free cyanide species to the gold surface, which follows Fick's first law of diffusive flux. The diffusion coefficient in liquid can be calculated with the Stokes-Einstein equation which is influenced by temperature and the component properties of the solute. The last rate determining step is the gold cyanidation on the surface

Table 1
Low-cost optical irradiance sensors compared.

	Photoactive	Change in conductivity	Direct electrical readout	Cumulative without logging	Advantages
Photochromic molecules	X ^a	–	–	X ^a	Simple visual readout
Photo conductive element	X ^b	X ^b	X ^c	–	Instant signal, quantitative
This work	X ^d	X ^c	X ^c	X ^f	Quantitative/cumulative without data logging

^a Photochromic molecules are known for their color changing capabilities upon light exposure. The change can be correlated with intensity or exposure time (cumulative) by making use of UV/VIS spectrometry [35–37].

^b Photo conductive elements including light dependent resistors, photodiodes, phototransistors and photovoltaic cells provide a signal upon illumination as a change in conductivity [38–41].

^c These elements can be wired in different ways for electrical readout. However, a data logger is required for cumulative measurement [42,43].

^d Photoactivity of potassium ferrocyanide has been confirmed in Fig. 1.

^e Change in conductivity and electrical readout is introduced in Fig. 2 with the influence of pH variation.

^f Cumulative light measurement is demonstrated in Fig. 5.

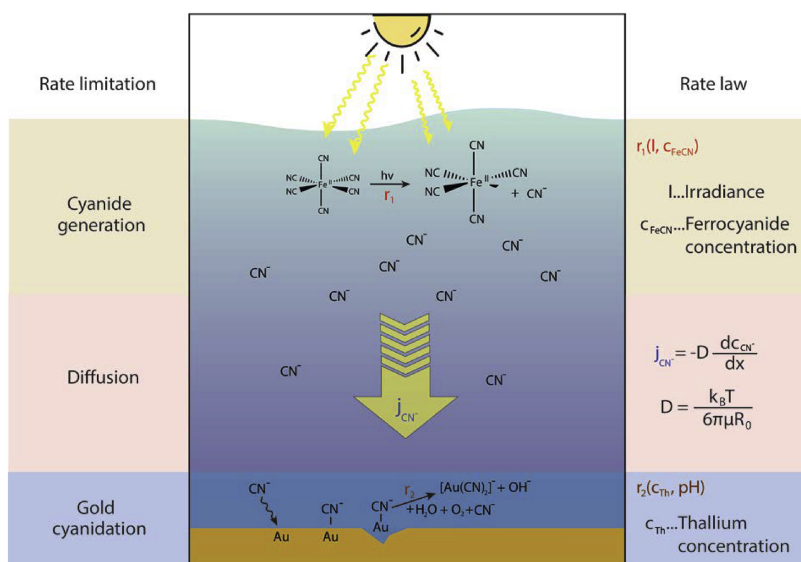


Fig. 6. The light triggered gold degradation system has been divided into three parts, which have all proven their influence in the conducted experiments. Cyanide generation being the first step in the process shows an irradiance and ferrocyanide concentration dependency. Diffusion time is described by Fick's law, which influences the reaction rate by the "supply rate" of free cyanide to the gold surface. Finally, the gold cyanidation rate is limited by the pH, which influences the solubility of the free cyanide species and the surface coverage of the adsorbed free cyanide can be influenced by adding the heavy metal thallium.

itself which, following our observations, is dependent on the pH of the solution and the surface coverage of cyanide ions and can be influenced with addition of the heavy metal thallium.

Using the final set of experiments (Fig. 5), we could calculate the light efficiency of this system, yielding a photon to the dissolved gold atom ratio of 38:1 (see Supporting Information for details and assumptions of calculation). Assuming each photon releases one cyanide ion from the ferrocyanide complex and accounting for the molar ratio of cyanide to gold (2:1), the efficiency of the light triggered gold dissolution process at an irradiance of 300 W m^{-2} and a thallium content of (260 ppb) is 2.56%.

4. Conclusions

We have demonstrated a light triggered cyanidation system to dissolve gold, which remains inactive in the dark. The gold cyanidation rate can be controlled by either varying pH, potassium ferrocyanide concentration, light intensity or the addition of the heavy metal thallium.

From a conceptual view the method can be seen as a device that transforms light into an electrical signal via a photochemical route, where the aqueous ferrocyanide solution acts as a "light-collecting" reservoir, converting photons to free cyanide ions. These then find their way to the gold electrode (diffusion), dissolving the gold and increasing the electrical resistance of the device in a quantitative manner.

The applicability of this photosensitive system as a cumulative light sensor device was also demonstrated. In contrast to conventional light sensing devices this device can be seen as an offline, zero-energy-demand (battery-free) sensor and integrator, which stores the signal as the thickness of the gold wire, and enables rapid signal readout (resistance measurement). This attribute enables the sensor to measure in situ, completely cut off from any connections, making it possible to measure light in remote or extensive areas with minimum infrastructure needed. It is believed that such sensing/integration/storage devices may further be useful in the Internet of Things (IoT), where sensor cost and construction simplicity is of uttermost importance [44]. Alternative applications of the method in the realm of transient electronics in quality assurance (making sure packages have not been exposed to any light source throughout the transport) and secured electronic circuits (device disintegrates upon illumination/opening of the device) are currently being actively pursued.

Conflicts of interest

The authors declare no competing financial interest.

Acknowledgment

We thank the Center for Micro and Nanoscience at ETH Zurich for the fabrication of the samples, in particular, Dr. Yargo Bonetti and Sandro Loosli.

Appendix A. Supplementary data

Supplementary data associated with this article can be found, in the online version, at <https://doi.org/10.1016/j.snb.2018.10.094>.

References

- [1] C.W. Park, S.-K. Kang, H.L. Hernandez, J.A. Kaitz, D.S. Wie, J. Shin, O.P. Lee, N.R. Sottos, J.S. Moore, J.A. Rogers, S.R. White, Thermally triggered degradation of transient electronic devices, *Adv. Mater.* 27 (2015) 3783–3788, <https://doi.org/10.1002/adma.201501180>.
- [2] H.L. Hernandez, S.-K. Kang, O.P. Lee, S.-W. Hwang, J.A. Kaitz, B. Inci, C.W. Park, S. Chung, N.R. Sottos, J.S. Moore, J.A. Rogers, S.R. White, Triggered transience of metastable poly(phthalaldehyde) for transient electronics, *Adv. Mater.* 26 (2014) 7637–7642, <https://doi.org/10.1002/adma.201403045>.
- [3] C.H. Lee, S.-K. Kang, G.A. Salvatore, Y. Ma, B.H. Kim, Y. Jiang, J.S. Kim, L. Yan, D.S. Wie, A. Banks, S.J. Oh, X. Feng, Y. Huang, G. Troester, J.A. Rogers, Wireless microfluidic systems for programmed, functional transformation of transient electronic devices, *Adv. Funct. Mater.* 25 (2015) 5100–5106, <https://doi.org/10.1002/adfm.201502192>.
- [4] S.-W. Hwang, J.-K. Song, X. Huang, H. Cheng, S.-K. Kang, B.H. Kim, J.-H. Kim, S. Yu, Y. Huang, J.A. Rogers, High-performance biodegradable/transient electronics on biodegradable polymers, *Adv. Mater.* 26 (2014) 3905–3911, <https://doi.org/10.1002/adma.201306050>.
- [5] S.H. Jin, J. Shin, I.-T. Cho, S.Y. Han, D.J. Lee, C.H. Lee, J.-H. Lee, J.A. Rogers, Solution-processed single-walled carbon nanotube field effect transistors and bootstrapped inverters for disintegratable, transient electronics, *Appl. Phys. Lett.* 105 (2014) 013506, <https://doi.org/10.1063/1.4885761>.
- [6] C. Dagdeviren, S.-W. Hwang, Y. Su, S. Kim, H. Cheng, O. Gur, R. Haney, F.G. Omenetto, Y. Huang, J.A. Rogers, Transient, biocompatible electronics and energy harvesters based on ZnO, *Small* 9 (2013) 3398–3404, <https://doi.org/10.1002/smll.201300146>.
- [7] S.-K. Kang, S.-W. Hwang, H. Cheng, S. Yu, B.H. Kim, J.-H. Kim, Y. Huang, J.A. Rogers, Dissolution behaviors and applications of silicon oxides and nitrides in transient electronics, *Adv. Funct. Mater.* 24 (2014) 4427–4434, <https://doi.org/10.1002/adfm.201304293>.
- [8] S.-K. Kang, S.-W. Hwang, S. Yu, J.-H. Seo, E.A. Corbin, J. Shin, D.S. Wie, R. Bashir, Z. Ma, J.A. Rogers, Biodegradable thin metal foils and spin-on glass materials for transient electronics, *Adv. Funct. Mater.* 25 (2015) 1789–1797, <https://doi.org/10.1002/adfm.201403469>.
- [9] S.-W. Hwang, G. Park, C. Edwards, E.A. Corbin, S.-K. Kang, H. Cheng, J.-K. Song, J.-H. Kim, S. Yu, J. Ng, J.E. Lee, J. Kim, C. Yee, B. Bhaduri, Y. Su, F.G. Omenetto,

- Y. Huang, R. Bashir, L. Goddard, G. Popescu, K.-M. Lee, J.A. Rogers, Dissolution chemistry and biocompatibility of single-crystalline silicon nanomembranes and associated materials for transient electronics, *ACS Nano*. 8 (2014) 5843–5851, <https://doi.org/10.1021/nn500847g>.
- [10] K.K. Fu, Z. Wang, J. Dai, M. Carter, L. Hu, Transient electronics: materials and devices, *Chem. Mater.* 28 (2016) 3527–3539, <https://doi.org/10.1021/acs.chemmater.5b04931>.
- [11] L. Yin, H. Cheng, S. Mao, R. Haasch, Y. Liu, X. Xie, S.-W. Hwang, H. Jain, S.-K. Kang, Y. Su, R. Li, Y. Huang, J.A. Rogers, Dissolvable metals for transient electronics, *Adv. Funct. Mater.* 24 (2014) 645–658, <https://doi.org/10.1002/adfm.201301847>.
- [12] K.V. Rajeshwari, Tackling E-waste: towards efficient management techniques, Teri, 2007.
- [13] Gold Demand Trends Q1 2017, (n.d.). <http://www.gold.org/> (accessed June 12, 2017).
- [14] W.C. Buttermann, E.B. Amey III, U.S. Geological Survey Open-File Report 02-303 - Mineral commodity profiles - gold, (2005) <https://pubs.usgs.gov/of/2002/of02-303/> (accessed June 12, 2017).
- [15] D.A. Dzombak, R.S. Ghosh, G.M. Wong-Chong, *Cyanide in Water and Soil: Chemistry, Risk, and Management*, CRC Press, Boca Raton, Florida, USA, 2005.
- [16] A.H. Hall, G.E. Isom, G.A. Rockwood, *Toxicology of Cyanides and Cyanogens: Experimental, Applied and Clinical Aspects*, John Wiley & Sons, Chichester, West Sussex, UK, 2015.
- [17] A.O. Gettler, *The Toxicology of Cyanide*, New York University (1938).
- [18] R. Eisler, *Cyanide Hazards to Fish, Wildlife, and Invertebrates: A Synoptic Review*, U.S. Department of the Interior, Fish and Wildlife Service, Washington D.C., Columbia, USA, 1991.
- [19] G. Eisenbrand, P. Schreier, *RÖMPP Lexikon Lebensmittelchemie 2 Auflage*, 2006, Georg Thieme Verlag, Stuttgart, Baden-Württemberg, Germany, 2014.
- [20] J.C.L. Meeussen, M.G. Keizer, F.A.M. De Haan, Chemical stability and decomposition rate of iron cyanide complexes in soil solutions, *Environ. Sci. Technol.* 26 (1992) 511–516, <https://doi.org/10.1021/es00027a010>.
- [21] F. Haber, Nachweis und Fällung der Ferroionen in der Wässerigen Lösung des Ferrocyanalkaliums, *Z. Für Elektrochem. Angew. Phys. Chem.* 11 (1905) 846–850, <https://doi.org/10.1002/bbpc.19050114709>.
- [22] S. Ašperger, Kinetics of the decomposition of potassium ferrocyanide in ultra-violet light, *Trans. Faraday Soc.* 48 (1952) 617–624, <https://doi.org/10.1039/TF9524800617>.
- [23] X.Z. Yu, X.Y. Peng, G.L. Wang, Photo induced dissociation of ferri and ferro cyanide in hydroponic solutions, *Int. J. Environ. Sci. Technol.* 8 (2011) 853–862, <https://doi.org/10.1007/BF03326268>.
- [24] H.F. Wasgestian, Photoaquotisierung von Hexacyanochromat(III)*, *Z. Für Phys. Chem.* 67 (2011) 39–50, <https://doi.org/10.1524/zpch.1969.67.1.3.039>.
- [25] P. Hummel, N.W. Halpern-Manners, H.B. Gray, Electronic excited states of tetracyanonickelate (II), *Inorg. Chem.* 45 (2006) 7397–7400, <https://doi.org/10.1021/ic060584r>.
- [26] S. Ellis, G. Senanayake, The effects of dissolved oxygen and cyanide dosage on gold extraction from a pyrrhotite-rich ore, *Hydrometallurg* 72 (2004) 39–50, [https://doi.org/10.1016/S0304-386X\(03\)00131-2](https://doi.org/10.1016/S0304-386X(03)00131-2).
- [27] P. Ling, V.G. Papangelakis, S.A. Argyropoulos, P.D. Kondos, An improved rate equation for cyanidation of a gold ore, *Can. Metall. Q.* 35 (1996) 225–234, <https://doi.org/10.1179/cm.1996.35.3.225>.
- [28] S.R. La Brooy, H.G. Linge, G.S. Walker, Review of gold extraction from ores, *Miner. Eng.* 7 (1994) 1213–1241, [https://doi.org/10.1016/0892-6875\(94\)90114-7](https://doi.org/10.1016/0892-6875(94)90114-7).
- [29] J. Marsden, I. House, *The Chemistry of Gold Extraction*, SME, Littleton, Colorado, USA, 2006.
- [30] M.J. Nicol, The anodic behaviour of gold, *Gold Bull.* 13 (1980) 46–55, <https://doi.org/10.1007/BF03215452>.
- [31] Y. Guan, K.N. Han, An electrochemical study on the dissolution of gold and copper from gold/copper alloys, *Metall. Mater. Trans. B* 25 (1994) 817–827, <https://doi.org/10.1007/BF02662764>.
- [32] T.P. Pan, C.C. Wan, Anodic behaviour of gold in cyanide solution, *J. Appl. Electrochem.* 9 (1979) 653–655, <https://doi.org/10.1007/BF00610956>.
- [33] Y. Yang, Q. Li, T. Jiang, Y. Guo, G. Li, B. Xu, Co-intensification of gold leaching with heavy metals and hydrogen peroxide, *Trans. Nonferrous Met. Soc. China*. 20 (2010) 903–909, [https://doi.org/10.1016/S1003-6326\(09\)60234-X](https://doi.org/10.1016/S1003-6326(09)60234-X).
- [34] P. Ineichen, Global irradiation: average and typical year, and year to year annual variability, (2011) <https://archive-ouverte.unige.ch/unige:23518> (accessed March 12, 2018).
- [35] D.G. Duff, R.S. Sinclair, D. Stirling, Light-induced colour changes of natural dyes, *Stud. Conserv.* 22 (1977) 161–169, <https://doi.org/10.2307/1505832>.
- [36] H.C.A. van Beek, Light-induced colour changes in dyes and materials, *Color Res. Appl.* 8 (1983) 176–181, <https://doi.org/10.1002/col.5080080309>.
- [37] S.A. Brewer, C.P. Artilles, J.A. Taylor, M. Dennis, Photosensitive dyes and self-detoxifying textiles: degradation products and dye durability, *Appl. Surf. Sci.* 256 (2010) 1908–1912, <https://doi.org/10.1016/j.apsusc.2009.10.033>.
- [38] A.S. Joshi, I. Dincer, B.V. Reddy, Performance analysis of photovoltaic systems: a review, *Renew. Sustain. Energy Rev.* 13 (2009) 1884–1897, <https://doi.org/10.1016/j.rser.2009.01.009>.
- [39] A.F. Gibson, The sensitivity and response time of lead sulphide photoconductive cells, *Proc. Phys. Soc. Sect. B* 64 (1951) 603, <https://doi.org/10.1088/0370-1301/64/7/308>.
- [40] E. Schwarz, New Photoconductive Cells, *Nature* 162 (1948) 614–615, <https://doi.org/10.1038/162614b0>.
- [41] E.S. Rittner, Concerning the theory of photoconductivity in infrared-sensitive semiconducting films, *Science* 111 (1950) 685–688, <https://doi.org/10.1126/science.111.2895.685>.
- [42] M.G.C. Peiris, I.K. Perera, A simple inexpensive photometer using light-dependent resistors, *Am. J. Phys.* 55 (1987) 1147, <https://doi.org/10.1119/1.15269>.
- [43] J.F. Cox, *Fundamentals of Linear Electronics: Integrated and Discrete*, Cengage Learning, Albany, New York, USA, 2002.
- [44] Goldman Sachs, Technology Driving Innovation - The Internet of Things: The Next Mega-Trend. Goldman Sachs (n.d.). <http://www.goldmansachs.com/our-thinking/pages/internet-of-things/> (accessed October 24, 2017).

Weida D. Chen completed his B.S. and M.S. in Chemical and Bioengineering from the Swiss Federal Institute of Technology Zurich, Switzerland, in 2010 and 2015. He is currently pursuing his Ph.D. degree with a research focus on transient electronics and DNA data storage.

Seung-Kyun Kang obtained B.S. and Ph.D. degrees in Materials Science and Engineering from the Seoul National University, Korea, in 2006 and 2012. He worked as a post-doctoral researcher at University of Illinois at Urbana–Champaign (2012–2016) and at Northwestern University (2016–2017). He joined the Department of Bio and Brain Engineering at KAIST as an Assistant Professor in 2017.

Wendelin Stark is Full Professor at the Institute for Chemical and Bioengineering of ETH Zurich and heads the chair in Functional Materials Engineering. He studied Chemistry at the ETH with a stay at the UC Berkeley in 1999 and pursued a Ph.D. in Mechanical and Process Engineering at ETH. Wendelin Stark develops nanomaterial-based solutions for industrial and medical markets. He has commercialized over 20 products and cofounded six companies.

John A. Rogers obtained B.A. and B.S. degrees in chemistry and in physics from the University of Texas, Austin, in 1989. He received S.M. degrees in physics and in chemistry (1992) and a Ph.D. in physical chemistry (1995) from MIT. Rogers was a Junior Fellow in the Harvard University Society of Fellows (1995–1997). He joined Bell Laboratories as a Member of Technical Staff in the Condensed Matter Physics Research Department (1997), and served as Director of this department (2000–2002). He spent 13 years on the faculty at the University of Illinois at Urbana–Champaign, most recently as the Swanlund Chair Professor. He currently holds the position of Louis Simpson and Kimberly Querrey Professor at Northwestern University with appointments in the Departments of Materials Science and Engineering and others, where he also serves as Director of the Center for Bio-Integrated Electronics.

Robert Grass is Titular Professor at the Functional Materials Laboratory at ETH Zurich. He studied Chemical Engineering at ETH with a stay at CASE Western Reserve University Cleveland in 2003 after which he pursued a Ph.D. at ETH Zurich. His research encompasses nanomaterial science, surface chemistry and nucleic acid research.